Z-cut Barium Titanate Modulator on a Silicon Photonic Platform

Vincent Stenger(1), John DeFouw(1), Agham Posadas(2), Alexander Demkov(2), Sri Sriram(1)

(1) SRICO, Inc., Columbus, OH, U.S.A., vestenger@srico.com
(2) Department of Physics, The University of Texas at Austin, Austin, TX, U.S.A

Abstract *Z-cut barium titanate modulator device structures were epitaxially integrated on silicon-on insulator wafers. Deposited films exhibited excellent structural quality with Pockels coefficient r_{33} >100 pm/V and propagation loss <2 dB/cm. Slot waveguide modulators in the material have potential for Vpi-length of 0.3 V-cm.*

Introduction

Silicon on insulator (SOI) is an excellent platform for photonic applications due to the ability to fabricate waveguides with very low losses and high optical mode confinement [1-2]. To capitalize on this, active electro-optic (EO) devices need to be readily manufacturable on silicon (Si) substrates.

While ferroelectric $LiNbO_3$ is well-established as an excellent material in terms of RF EO gain-bandwidth, linearity, low optical loss, and overall robustness [3-4], it is not straightforward to integrate high quality material with silicon [5].

$BaTiO_3$ (BTO) is another ferroelectric material that exhibits one of the largest Pockels coefficients among EO materials, as high as 1300 pm/V in the bulk [6]. In addition to the substantially larger Pockels coefficient compared to $LiNbO_3$, BTO is much easier to integrate with Si [7-9]. This makes epitaxial BTO on Si a promising materials platform for compact high speed and low power analog EO modulators, optical switches, or even for new forms of computing including neuromorphic and quantum computing [10].

Mach-Zehnder and ring resonator hybrid modulators based on Si waveguides patterned on top of BTO on silicon have been demonstrated by Eltes et al. [11] and Xiong et al. [12], respectively. These devices demonstrate that substantial EO modulation can be achieved in Si photonics-compatible processes. In both cases, the devices utilized a portion of the r_{42} component of the BTO Pockels tensor, which is the largest component and relies on the BTO film having its ferroelectric polarization in-plane (a-axis oriented or X-cut films).

While the r_{42} coefficient represents the largest EO coefficient in BTO, fields applied along the X-direction of the crystal to access this coefficient experience an extremely high dielectric constant, typically over 1000. This high dielectric constant directly translates to decreased EO modulation efficiency. In contrast, fields applied along the Z direction to access the r_{33} Pockels component experience a typical BTO dielectric constant less than 60. For high-speed modulator devices, this reduction in dielectric loading can more than offset the reduction in EO coefficient. Another benefit to Z-cut films is that they may readily be poled along the surface normal direction to produce a uniform poled BTO material across the wafer. That is, the material can be formed as a continuous single domain layer. This contrasts with the multiple oriented domains found in X-cut films. The combination of reduced dielectric loading and uniform single domain structure provides motivation for Z-cut EO modulator devices based on r_{33}.

Thin Film Growth

Standard photonic-grade SOI wafers from Soitec were used as the substrate for BTO thin film growth. The wafers were cored to 2” diameter, degreased in acetone, isopropanol, and deionized water, then dried and exposed to UV/ozone to decompose organic contaminants.

After loading into the deposition chamber, the wafers were first outgassed at 700°C in ultrahigh vacuum, then the native oxide was desorbed using Sr-assisted deoxidation [13]. One-half monolayer of Sr metal was deposited at 600°C to form a protective layer on Si prior to the next step.

Before BTO deposition, an 8-nm thin $SrTiO_3$ (STO) buffer layer was deposited on the Si in two steps by molecular beam epitaxy (MBE). A 2 nm seed layer was grown at 200°C and vacuum annealed at 550°C for 5 min, followed by growth of 6 nm STO at 550°C under $4x10^{-7}$ Torr oxygen.

After STO buffer formation, the wafer was transferred *in situ* to an RF sputtering system for BTO growth. BTO was deposited to a thickness of 110 nm at a power density of 2.2 W/cm^2 in a 3:7 O_2:Ar mixture at a total pressure of 10 mTorr. The system had an off-axis geometry where the substrate normal axis was 90° from the sputtering gun axis. Deposition was done at a substrate temperature of 680°C and the sample was cooled down at 5°C/min to room temperature. Typical growth rates were ~2 nm/min.

Structural Characterization

Grown BTO samples were measured using *in situ* reflection high energy electron diffraction (RHEED) and *in situ* X-ray photoelectron spectroscopy prior to being unloaded from the vacuum system. Results indicated a very flat and highly ordered crystalline surface.

Samples were then analysed using X-ray diffraction to determine in-plane and out-of-plane lattice constants. The measurements were performed using a Rigaku Ultima IV diffractometer with in-plane arm using Cu Kα radiation. Fig. 1 shows scans along the out-of-plane and in-plane 002/200 directions. Data analysis indicated an out-of-plane lattice constant of 4.035 Å and an in-plane lattice constant of 4.004 Å, confirming the material to be c-axis (Z-cut) oriented with c/a ratio = 1.007742. Rocking curve scans in the out-of-plane direction showed typical full width at half-maximum values of 0.6°. The STO buffer layer was also evident in the out-of-plane scan. X-ray reflectivity data was gathered to confirm the layer thicknesses. Based on the reflectivity data, the BTO thickness was 106.9 nm and the STO thickness was 8.1 nm. Surface roughness was determined to be 0.4 nm.

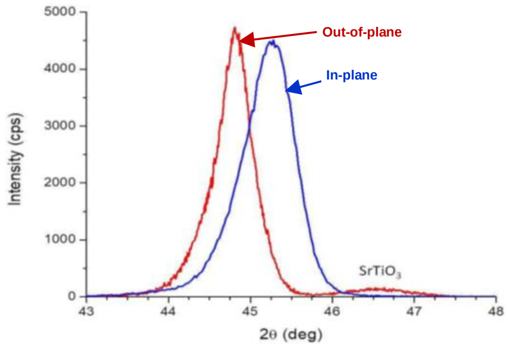

Fig. 1: In-plane and out-of-plane X-ray diffraction scans of a BTO film on an SOI wafer showing c-axis oriented (Z-cut) film.

Slab Mode Characterization

The refractive index for the Z-cut BTO films grown on SOI wafers was characterized over visible and near-infrared wavelengths via variable angle spectroscopic ellipsometry. The resulting index value was 2.280 at 1550 nm. This result was in line with values reported for optical grade BTO films.

Slab waveguide loss testing was done using a Metricon 2010 prism coupler measurement system with optical loss attachment. Slab loss was measured to be in the range of 1 to 1.5 dB/cm for both transverse electric (TE) and transverse magnetic (TM) polarization modes at 1550 nm wavelength. This result confirmed that the material would be suitable for implementation of Mach Zehnder modulator (MZM) devices.

The Metricon system was also used to test EO modulation of the BTO film. For this test, the system was set up so that incident light partially coupled into the fundamental slab mode. Modulation of the BTO index was achieved by applying a voltage across the wafer sample, as shown in Fig. 2. The sputter deposited Si layer served as an optically transparent electrode. The electric field applied across the BTO thickness was modelled by assuming a simple 1D layer stack-up in which the Si layers were partially conductive dielectrics and the BTO and SiO_2 layers were pure dielectrics. BTO was assumed to have a dielectric constant of 56 in the surface normal (Z) direction [14]. Slab test results indicated an r_{33} value between 100 and 120 pm/V, which was slightly higher than that for bulk BTO crystal [14].

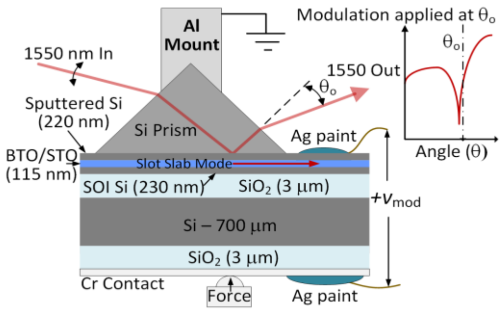

Fig. 2: Electro-optic r_{33} measurement using a prism coupling configuration.

Electro-optic Modulator Test Device

Slab modulation tests were done at audio frequencies due to limitations of the prism coupler electronics. TM mode MZM test devices were subsequently designed and fabricated to test the radio frequency (RF) response of the Z-cut BTO material. The test device cross section design is shown in Fig. 3. This geometry was relatively simple to produce as it only required three process steps: ridge etch, oxide deposition, and electrode patterning. Multimode interference (MMI) splitters were also designed to implement the splitter portions of the MZM device.

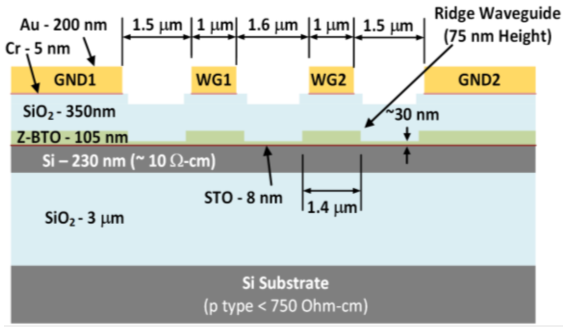

Fig. 3: Cross sectional geometry of the Z-cut MZM test device in the modulation section.

Device fabrication process steps entailed patterning and wet etching the BTO ridge in a Nitric based acid solution, followed by plasma enhanced chemical vapor deposition (PECVD) of SiO_2 to a thickness of 350 nm. Electrodes were formed using a maskless patterning and lift-off process. An optical microscope image of a completed MZM test device is shown in Fig. 4.

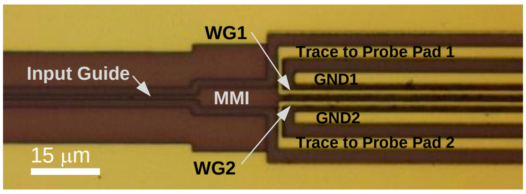

Fig. 4: Launch section of the fabricated Z-cut MZM test device.

TM polarized EO measurements were taken by modulating one waveguide electrode while holding the other at ground. Equal amplitude and opposite phase were observed in the MZM EO responses for the two waveguide electrodes, indicating equal EO coefficients for the waveguides. This further indicated the BTO layers were equally and uniformly poled along the same crystal direction.

To quantify the EO performance, a triangle wave was injected into one of the waveguide electrodes of a 1 mm length MZM test device. From Fig. 5, a 3.105 Vpp linear modulation produced a 346.2 mVpp linear output. The electric field drop across the SiO_2 buffer resulted in a Vpi that was too high to measure by full sweeping of the MZM characteristic. Instead, quadrature bias conditions were confirmed through lock-in amplifier measurements of 1st and 2nd order modulation products.

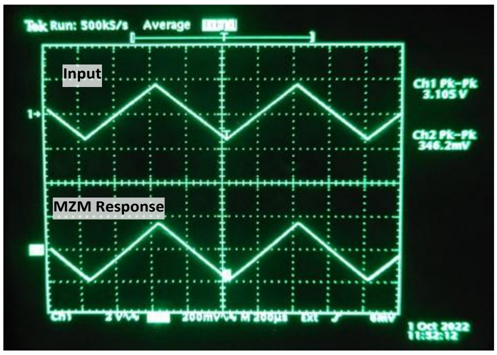

Fig. 5: Linear EO response of the Z-cut MZM test device.

The EO coefficient (r_{33}) was calculated from the measured modulation response through simulation of EO overlap between the applied electric field and the optical mode in the BTO, as well as the sensitivity of the propagating mode to the BTO material index. The r_{33} value was extracted to be 134.4 pm/V. This value was consistent, albeit slightly higher than that measured through the slab waveguide EO tests.

RF modulation testing was nominally done at 20 MHz and was limited by the test probe pad lumped capacitances to less than 1 GHz for a 50Ω source. Responses were observed to be relatively flat over RF frequency, with no fine or resonant mode spectral features being observed.

High efficiency Z-cut BTO Modulator Design

An efficient EO modulator may be implemented in the Z-cut BTO material as shown by the simulation result in Fig. 6. For this slot waveguide configuration, most of the optical mode is in the BTO layer. An additional 350 nm of high-k a-oriented BTO is placed on top of the stack to provide optical isolation from the metal electrode while maintaining dielectric continuity through the active BTO layer. TM mode propagation is used to access r_{33}. Based on measured loss and EO coefficients for the Z-cut BTO and mode overlap calculations, a "push-pull" MZM device based on such a structure can achieve a Vπ-L value of about 0.3 V-cm. This makes the sputter grown Z-cut BTO material a rather promising candidate for high density integrated RF photonics.

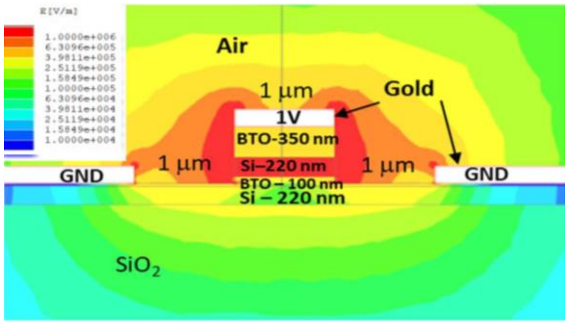

Fig. 6: Quasistatic electric field simulation for a Z-cut BTO slot waveguide optical phase modulator design.

Conclusions

Electro-optic grade BTO was grown in a Z-cut configuration on SOI substrates via a high-speed sputter deposition process. Measured slab mode optical losses were on order of 1 dB/cm for both TE and TM modes. Electro-optic measurements indicated an r_{33} value comparable to bulk BTO. An integrated optic modulator device design based on the BTO material indicated potential for 0.3 V-cm performance. RF response was flat and limited primarily by RF pad capacitances. Low capacitance pads may be implemented for RF EO testing to > 60 GHz.

Acknowledgements

This work was done under support of U.S. Air Force contract number FA864920C0336. The views expressed are those of the authors and do not reflect the official policy or position of the Department of Defense or the U.S. Government.

References

[1] G. T. Reed, G. Mashanovich, F. Y. Gardes, and D. J. Thomson, “Silicon optical modulators,” Nature Photonics, vol. 4, p. 518, 2010. DOI: 10.1038/nphoton.2010.179

[2] S. Abel and J. Fompeyrine, “Electro-optically active oxides on silicon for photonics,” in Thin Films on Silicon, edited by V. Narayanan, M. Frank, and A. A. Demkov (World Scientific, Singapore, (2016), pp. 455-501, DOI: 10.1142/9908 .

[3] V.E. Stenger, J. Toney, A. Pollick, D. Brown, B. Griffin, R. Nelson, and S. Sriram, "Low Loss and Low Vpi Thin Film Lithium Niobate on Quartz Electro-optic Modulators," European Conference on Optical Communication, 2017. DOI: 10.1109/ECOC.2017.8346144

[4] M. Zhang, C. Wang, P. Kharel, D. Zhu, and M. Lončar, "Integrated lithium niobate electro-optic modulators: when performance meets scalability," Optica vol. 8, p. 652, 2021. DOI: 10.1364/OPTICA.415762

[5] P. Rabiei, J. Ma, S. Khan, J. Chiles, and S. Fathpour, “Heterogeneous lithium niobate photonics on silicon substrates,” Optics Express, vol. 21, p. 25573, 2013. DOI: 10.1364/OE.21.025573

[6] W. Guo, A.B. Posadas, and A.A. Demkov, "Epitaxial integration of $BaTiO_3$ on Si for electro-optic applications", Journal of Vacuum Science & Technology A vol. 39, 030804, 2021. DOI: 10.1116/6.0000923

[7] S. Abel, T. Stöferle, C. Marchiori, C. Rossel, M.D. Rossell, R. Erni, D. Caimi, M. Sousa, A. Chelnokov, B.J. Offrein, and J. Fompeyrine. "A strong electro-optically active lead-free ferroelectric integrated on silicon," Nature Communications, vol. 4, p. 1671, 2013. DOI: 10.1038/ncomms2695

[8] A.A. Demkov and A.B. Posadas, Integration of Functional Oxides with Semiconductors, (Springer, Berlin, 2014), pp.187-195 DOI: 10.1007/978-1-4614-9320-4

[9] A.B. Posadas, H. Park, M. Reynaud, W. Cao, J.D. Reynolds, W. Guo, V. Jeyaselvan, I. Beskin, G.Z. Mashanovich, J.H. Warner, and A.A. Demkov, "Thick $BaTiO_3$ Epitaxial Films Integrated on Si by RF Sputtering for Electro-Optic Modulators in Si Photonics," ACS Applied Materials & Interfaces vol. 13, p. 51230, 2021. DOI: 10.1021/acsami.1c14048

[10] A.A. Demkov, C. Bajaj, J.G. Ekerdt, C.J. Palmstrøm, and S.J.B. Yoo, "Materials for emergent silicon-integrated optical computing", Journal of Applied Physics vol. 130, 070907, 2021. DOI: 10.1063/5.0056441

[11] F. Eltes, C. Mai, D. Caimi, M. Kroh, Y. Popoff, G. Winzer, D. Petousi, S. Lischke, J.E. Ortmann, L. Czornomaz, L. Zimmermann, J. Fompeyrine, and S. Abel, "A $BaTiO_3$-Based Electro-Optic Pockels Modulator Monolithically Integrated on an Advanced Silicon Photonics Platform," Journal of Lightwave Technology, vol. 37, p. 1456, 2019. DOI: 10.1109/JLT.2019.2893500 [12] C. Xiong, W.H.P. Pernice, J.H. Ngai, J.W. Reiner, D. Kumah, F.J. Walker, C.H. Ahn, and H.X. Tang, "Active Silicon Integrated Nanophotonics: Ferroelectric BaTiO3 Devices, " Nano Letters vol. 14, p. 1419, 2014. DOI: 10.1021/nl404513p

[12] C. Xiong, W.H.P. Pernice, J.H. Ngai, J.W. Reiner, D. Kumah, F.J. Walker, C.H. Ahn, and H.X. Tang, "Active Silicon Integrated Nanophotonics: Ferroelectric $BaTiO_3$ Devices, " Nano Letters vol. 14, p. 1419, 2014. DOI: 10.1021/nl404513p

[13] H. Li, X. Hu, Y. Wei, Z. Yu, X. Zhang, R. Droopad, A. A. Demkov, J. Edwards Jr., K. Moore, and W. Ooms, "Two-dimensional growth of high-quality strontium titanate thin films on Si," Journal of Applied Physics vol. 93, p. 4521. DOI: 10.1063/1.1562001

[14] M. Zgonik, P. Bernasconi, M. Duelli, R. Schlesser, P. Günter, M. H. Garrett, D. Rytz, Y. Zhu, and X. Wu, "Dielectric, elastic, piezoelectric, electro-optic, and elasto-optic tensors of $BaTiO_3$ crystals," Physical Review B, vol. 50, p. 5941, 1994. DOI: 10.1103/PhysRevB.50.5941